Review Article

Myocardial Perfusion

Juerg Schwitter, MD[1–3]*

Noninvasive cardiac magnetic resonance (CMR) imaging has progressed rapidly over the past few years and will most likely become an integral part of the diagnostic workup of patients with known or suspected coronary artery disease (CAD). In this article the rationale for using perfusion-CMR is discussed, followed by a summary of current state-of-the-art perfusion-CMR techniques that addresses pharmacological stress, monitoring, pulse sequences, and doses of contrast media (CM) for first-pass studies. In the second part, unresolved aspects of perfusion-CMR, such as the lack of fully established and validated imaging protocols, are discussed. The optimum pulse sequence parameters, required cardiac coverage, analysis algorithms, criteria for data quality, and other aspects remain to be defined. Furthermore, since expertise in perfusion-CMR is not yet widely available, training of physicians and technicians to perform perfusion-CMR according to recognized standards is an important future requirement. In the last part of the review, some ideas are proposed to improve the management of patients with known or suspected CAD. This involves making a shift from a "reactive" strategy, in which patients are typically approached when they are symptomatic, to an "active" strategy, in which perfusion-CMR is performed for early detection of high-risk patients so that revascularizations can be performed before potentially deadly infarcts occur. An ideal test for such an active strategy would be highly accurate, reliable, safe (and thus repeatable), and affordable. Large multicenter trials have shown that in experienced centers perfusion-CMR is reliable and repeatable, and it is hoped that future studies will demonstrate its cost-effectiveness as well.

Key Words: cardiac magnetic resonance; myocardial perfusion; contrast media; coronary artery disease; vasodilation
J. Magn. Reson. Imaging 2006;24:953–963.

THERE IS GENERAL AGREEMENT that the classic risk factors are most important for initiation and promotion of atherosclerosis (1). Once atherosclerosis is established, the vulnerability of an individual plaque can cause sudden rupture, which in a "vulnerable blood environment" can progress to thrombosis and infarction. In recent years our knowledge about plaque pathophysiology has increased tremendously and some characteristics of high vulnerability have been defined (Table 1) (2). While smaller retrospective studies suggested that nonhemodynamically significant plaques are particularly prone to rupture (3–5), they also showed that short-term risk is associated with higher-degree stenoses (5). Larger invasive studies from the pre-interventional era confirmed a very low risk of occlusions at the site of low-degree stenoses (6) compared to a high risk for rupture of high-grade stenoses when occlusion rates were considered over one to two years (7–10). If vulnerability would be determined by plaque composition irrespectively of plaque mass or degree of stenosis, one would expect similar complication rates in populations with and without ischemia. However, this is not the case according to the results of scintigraphic studies, which clearly demonstrate an increasing risk of complications along with increasing ischemic burden (11). Following these lines of evidence from large invasive and scintigraphic studies, it might be equivalent to assess stenosis severity by coronary MR angiography (MRA) or perfusion–cardiac magnetic resonance (CMR). Here, some technical aspects merit consideration. Given a 3-mm coronary vessel imaged with the currently available spatial resolution of 0.5×0.5 mm^2 for coronary MRA, signal distribution in as little as 27 pixels would determine the degree of stenosis. With respect to plaque composition and morphology, as little as six pixels per component would characterize a plaque causing a 70% luminal reduction (considering three components in the plaque: fibrosis, lipid necrotic core, and inflammatory cell-rich component, with each occupying a third of the plaque area). Alternatively, for myocardial perfusion assessment a 3-mm vessel is assumed to supply approximately 60 g of muscle tissue (12), which corresponds to about 10,500 pixels (considering a spatial resolution for perfusion imaging of 3×3 mm^2 and a cardiac coverage of 50%). It seems obvious that a change in stenosis severity would be more reliably detected by interrogating 10,500 pixels in the myocardium than 27 pixels covering the cross-sectional area of the coronary vessel. There is the potential that luminal narrowings can be reliably detected by coronary MRA with further improvements in hardware and

[1]Cardiology Clinics, University Hospital Zurich, Zurich, Switzerland.
[2]Cardiac MR Center, University Hospital Zurich, Zurich, Switzerland.
[3]Children's University Hospital, Zurich, Switzerland.
*Address reprint requests to: J.S., University Hospital Zurich, Cardiology Clinics, Raemistrasse 100, CH-8091 Zurich, Switzerland.
E-mail: juerg.schwitter@usz.ch
Received November 3, 2005; Accepted July 28, 2006.
DOI 10.1002/jmri.20753
Published online 11 October 2006 in Wiley InterScience (www.interscience.wiley.com).

Table 1
Major Criteria of Vulnerable Plaques*

1	Active inflammation (monocyte/macrophage and sometimes T-cell infiltration)
2	Thin cap with large lipid core
3	Endothelial denudation with superficial platelet aggregation
4	Fissured plaque
5	Stenosis > 90%

*According to Naghavi et al (2).

software, while it appears considerably more difficult to achieve a reliable characterization of plaque components in coronary artery lesions in the near future.

MYOCARDIAL PERFUSION ASSESSMENT BY CMR

The most commonly used approaches for perfusion-CMR utilize contrast media (CM) first-pass techniques. Alternatively, blood oxygen level-dependent (BOLD) techniques and spin-labeling techniques have also been applied to assess myocardial perfusion. Since the latter two approaches are still in an early experimental stage, the following description will focus on contrast-enhanced first-pass techniques. Several requirements must be met by these first-pass techniques in order to generate data sets from which relevant perfusion information can be derived: 1) high temporal resolution of data acquisition (entire stack of images every one to two heartbeats) to provide unsmoothed signal intensity–time curves, 2) high spatial resolution to differentiate transmural differences in perfusion, 3) adequate cardiac coverage to assess the extent of disease, and 4) CM sensitivity to achieve an adequate contrast-to-noise ratio (CNR, i.e., T_1 or T_2* weighting corresponding to the type and dose of CM). These requirements must be met during hyperemic conditions.

Induction of Myocardial Hyperemia

Similarly to protocols used for single photon emission computed tomography (SPECT) perfusion imaging, hyperemia during perfusion-CMR is typically induced by intravenous administration of adenosine at a dose of 0.14 mg/kg/minute over three minutes. Adenosine acts via activation of adenylate cyclase through A_2 receptors on smooth muscle cells. Therefore, caffeine intake (from coffee, tea, and some chocolates) before the administration of adenosine blocks its effect, and these products should be avoided 24 hours before a perfusion-CMR study. This condition is usually not met in an emergency situation; however, in an acute setting, even resting perfusion is expected to be compromised. During hyperemia normal myocardial perfusion reaches 3–4 mL/min/g. Hemodynamically significant stenoses prevent an increase in perfusion toward these values. Instead, critical stenoses restrict perfusion to resting levels (approximately 1 mL/min/g), which are recognized as altered CM kinetics. As demonstrated in animal experiments, hyperemia very rarely causes a reduction in perfusion below resting values in stenosis-dependent myocardium, which would cause ischemia with consequent wall motion abnormalities (13). This may be the main reason why adenosine infusion is safe, as demonstrated in large SPECT registries (14). In line with these data, it was shown in the early 1990s that ischemia (by adrenergic stimulation), but not pure hyperemia, should be induced if dysfunction is used as the marker for CAD (15). Also, in large multicenter trials, adenosine in combination with CMR was proven safe (16–18). In a large SPECT registry (14), first- and second-degree AV-blocks occurred in 6.8% of patients, and third-degree AV-block occurred in 0.8%, all of which were transient (three-quarters of them even during continued adenosine infusion). Monitoring of the patient for symptoms, blood pressure, respiration, and cardiac rhythm is required during hyperemia by means of MR-compatible equipment. Since hypotension and asthma or bronchospasm may occur, all medications and devices for emergency treatment, including a defibrillator and adequate expertise in basic and advanced life support, must be available at the CMR site.

Since adenosine-induced hyperemia is regularly associated with high heart rates, very fast pulse sequences are required to meet the four requirements mentioned above.

Pulse Sequences for Perfusion-CMR

Turbo Fast Low-Angle Shot (FLASH) Sequences

In Turbo-FLASH pulse sequences the acquisition of each *k*-line is preceded by an RF excitation, which results in a readout duration on the order of 350–450 msec depending on the number of phase-encoding steps used and the duration of the TR, which is typically on the order of several milliseconds (19–24). Thus, turbo-FLASH sequences provide lower spatial and/or temporal resolution in comparison with hybrid echo-planar pulse sequences (25).

Echo-Planar or Hybrid Echo-Planar Pulse Sequences

In echo-planar pulse sequences, several *k*-lines are acquired following one single RF excitation, which reduces the TR per *k*-line down to <2 msec. This pulse design has been validated in larger trials with good results (16,17,26), and therefore is currently the method of choice. In order to reduce motion-induced artifacts, ideally the acquisition windows should be fitted into the cardiac cycle in such a way as to select phases with minimal motion (e.g., mid-diastole and/or mid- to end-systole) while optimizing the delay time. Figure 1 illustrates how this can be achieved.

Steady-State Free Precession (SSFP) Sequences

SSFP strategies preserve magnetization and therefore yield a higher signal-to-noise ratio (SNR). However, a preceding magnetization preparation, e.g., by a saturation pulse, limits the available magnetization and the magnetization preservation by SSFP appears less efficient. Accordingly, saturation-recovery SSFP yielded a contrast-to-noise ratio (CNR) of 6–8 after injection of 0.015 mmol/kg Gd-DTPA, which was not different from a turbo-FLASH acquisition (27). Furthermore, in general the readout for SSFP strategies for a given matrix is longer than that for echo-planar sequences, and com-

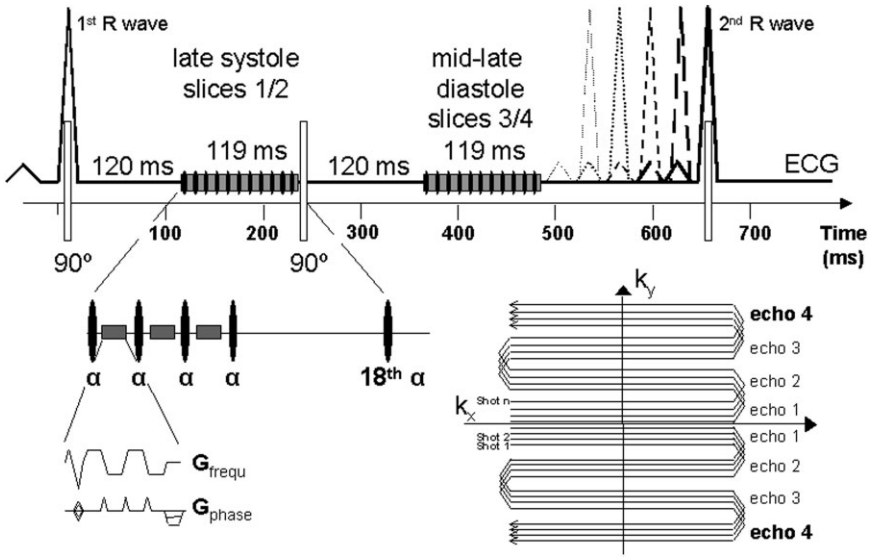

Figure 1. Pulse sequence diagram of a hybrid echo-planar approach as utilized in a recent study (26). A series of 50° α-pulses are played out, each of which yields four gradient echoes, i.e., four lines in *k*-space (as shown for *N* shots in the lower right corner of the figure). Each slice is prepared by a non-slice-selective 90° saturation pulse, followed by a delay time of 120 msec. With these parameters the readout occurs at phases of minimal cardiac motion, i.e., in late systole and mid-late diastole. This approach takes advantage of the fact that ejection time varies little with increasing heart rates, as is the case during adenosine-induced hyperemia (represented by the shift of the second R-wave on the ECG). A short readout is also crucial for avoiding data collection for slices 1 and 2 during early LV filling, and for slices 3 and 4 during atrial contraction (see p-wave on the ECG). Reprinted with permission from Ref. 70.

bination with magnetization preparation is not trivial with these sequences (28).

Parallel Imaging Approaches

Parallel imaging techniques are attractive because they allow for shortening the acquisition window by a factor of 2 or higher. However, a disadvantage is their reduced SNR (given by the square root of the acceleration factor times the so-called geometry factor) (29). Kellman et al (30) showed that such parallel imaging limitations can be overcome by meticulous optimization of other imaging parameters. Thus, combining temporal sensitivity encoding (TSENSE) with unaliasing by fourier encoding the overlap using the temporal dimension (UNFOLD) reconstruction yielded an up to 400% signal increase after injection of 0.1 mmol/kg of a Gd-chelate (CNR = ~18), whereas Auto-SENSE obtained a 50% signal change at 0.025 mmol/kg of Gd-chelate (31). Further studies are needed to determine whether the advantage of a shorter acquisition window with parallel imaging, which is likely to reduce motion-induced artifacts and/or increase cardiac coverage, improves diagnostic performance in unselected patient populations.

Magnetization Preparation for T_1-Shortening CM

Typically the readout is prepared by a 90° saturation pulse with recovery times as short as 100–150 msec. When combined with a hybrid echo-planar pulse sequence, the data acquisition window can be as short as 200–300 msec/slice (including preparation), allowing for multislice data acquisition at a high sampling rate, i.e., a complete stack of images can be acquired every one to two heartbeats (26). This preparation scheme has replaced the inversion recovery (IR) approach at most sites. With the IR technique the recovery time is set to null the signal of normal myocardium and is typically in the range of 300–400 msec (19–24). Thus, combining an IR-preparation scheme with a turbo-FLASH readout would result in long acquisition windows.

CM For Perfusion-CMR

T1-Shortening CM

Extravascular gadolinium (Gd)-based CM. Gd-based compounds are most commonly used for first-pass perfusion MRI. These CMs are injected as a bolus in a peripheral (antecubital) vein in doses of 0.025–0.15 mmol/kg body weight at rates of 3–8 mL/second. During CM administration the signal intensity changes in the right (RV) and left ventricular (LV) cavities and finally in the LV myocardium are monitored using one of the above-mentioned pulse sequences. The increase in signal during the first pass that is achieved in the LV myocardium depends on the dose and dispersion of the CM bolus, as well as the type of pulse sequence used. It appears crucial to induce a signal increase that is far higher than the noise floor in the images in order to be able to differentiate normally perfused myocardium from areas of hypoperfusion (32). An example of a perfusion-CMR study in a patient with atypical chest pain is shown in Fig. 2. Also, single-center (26,32) and multicenter (16,18) trials indicate a trend toward better diagnostic performance at higher doses of CM, at least when quantitative analyses of perfusion-linked param-

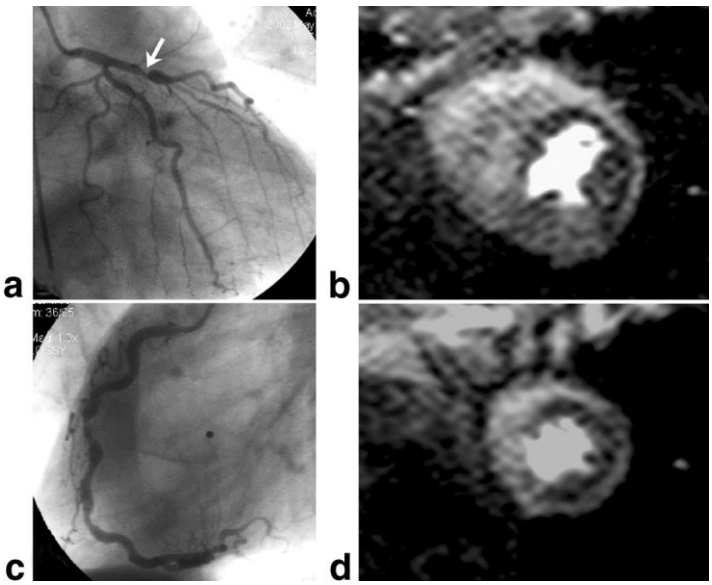

Figure 2. Example of a 67-year-old patient with walking-through angina. The first-pass perfusion study shows a large subendocardial perfusion deficit during adenosine-induced hyperemia in the anteroseptal and anterolateral walls (**b**) corresponding to a severe stenosis in the left anterior descending (LAD) coronary artery proximal to the take-off of large septal and diagonal branches (arrow in **a**). In a more apical slice, perfusion is also diminished in the lateral wall (**d**) corresponding to the territory of the large diagonal branches (a). In the apical slice, more than 50% of the LV wall is hypoperfused, indicating that fewer collaterals are supplying this portion of the LAD territory. With respect to the transmurality of perfusion deficits, it should be kept in mind that signal changes in the trabeculae and the papillary muscles should not be considered, since susceptibility artifacts are typically encountered in these structures, which are almost completely (circumferentially) exposed to the high CM concentrations in blood during first-pass conditions. Alterations in the right coronary artery (**c**) are not yet hemodynamically relevant.

eters, such as the upslope, are applied (Fig. 3a). Gd-BOPTA transiently binds to macromolecules, which increases its relaxivity in blood. Alternatively, a higher concentration of Gd-chelates is available for Gadobutrol (1 mmol/mL). Gd-BOPTA or Gadobutrol could help to reduce the CM dose and/or injection rate for first-pass perfusion imaging. However, conventional Gd-chelates (at 0.5 mmol/l) yielded a high diagnostic performance at injection rates of 5–8 mL/second using a peripheral IV line, which were shown to be safe in multicenter trials (16–18).

While doses up to 0.15 mmol/kg of Gd-DTPA yield an increase in subendocardial signal during the first pass (16), at very high concentrations of Gd-chelates in blood and tissue, T_2* effects begin to dominate and the first pass of CM at high doses and/or high injection rates could even result in a signal drop in the ventricular cavities and the myocardium (33). Pulse sequences

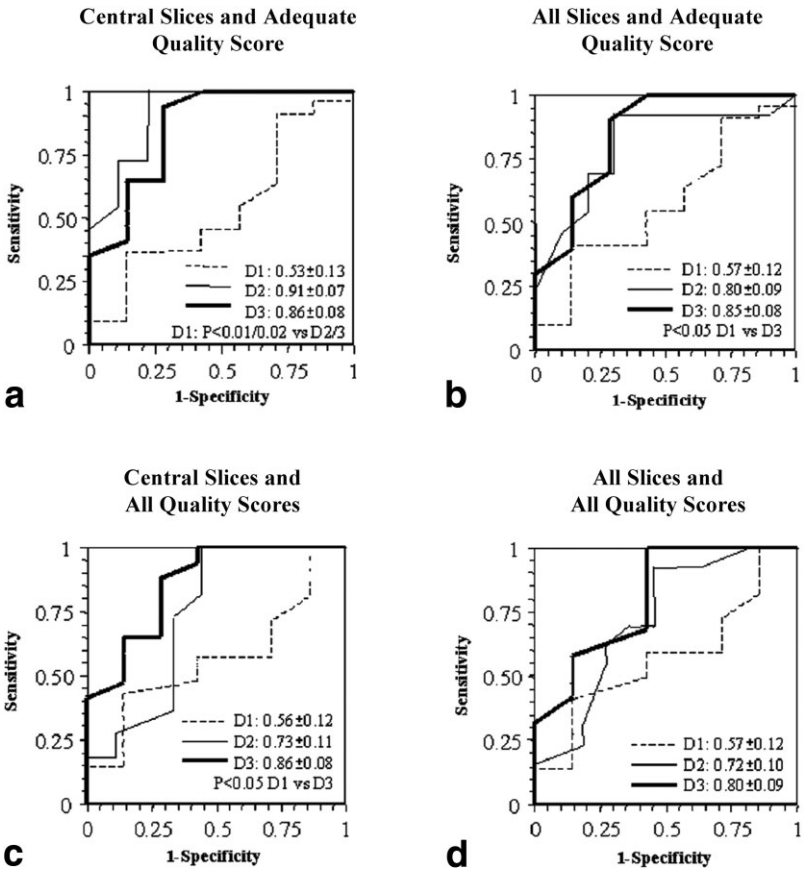

Figure 3. ROC curves of the MR upslope data of the subendocardial layer are shown for the detection of CAD (≥50% diameter reduction in at least one vessel by quantitative coronary angiography). When analysis is restricted to the data of adequate quality (approximately 85% of all studies) and the central three short-axis slices, which are acquired predominantly in phases of minimal cardiac motion (**a**), perfusion-CMR is highly reliable for detecting CAD with doses of CM (Gd-DTPA) of 0.10 and 0.15 mmol/kg (D2 and D3, respectively). The diagnostic performance (i.e., the AUC) is low for 0.05 mmol/kg (D1). The AUC for D2 and D3 diminishes for less restrictive data (**b** and **c**), and is worst when all data are included in the analysis (all qualities and all slices (**d**)). For D1, AUC is poor for all conditions (a–d). Reprinted with permission from Ref. 16.

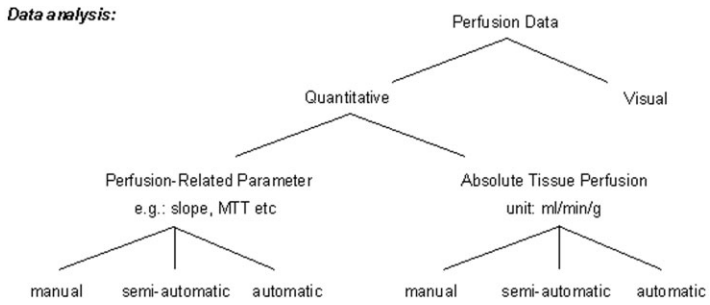

Figure 4. Perfusion data can be assessed in many ways, and some inconsistency is noted when analysis procedures are reported. A scheme is proposed for better definition of possible analysis strategies. In this scheme, "quantitative" means that results are obtained in numbers. This allows for better comparisons of research results (to define the best analysis algorithms) and individual examinations in a given patient both in cross section (e.g., patient data vs. normal database) and longitudinally (e.g., monitoring disease activity). Such quantitative results can be obtained manually (and thus are associated with some observer dependence) or semiautomatically (i.e., some observer interaction with the data set is present), or quantitative data can be obtained automatically, thus eliminating any observer interaction (i.e., analysis variability).

with longer TEs are particularly prone to T_2* effects and susceptibility artifacts at structures with high gradients in CM concentration (e.g., at the subendocardium–blood pool interface).

Intravascular Gd-based CM. Limited data are available regarding the application of intravascular Gd-based CM for myocardial perfusion imaging. To become an intravascular agent, Gd-ions are bound covalently to larger molecules, such as dendrimers (34), or Gd-chelates can bind transiently to large intravascular molecules, as is the case for MS-325, which binds to albumin (35). Since the molecular tumbling rate of these macromolecules is lower than that for the small Gd-chelates, relaxivity increases. If full relaxation (between RF pulses) of the intravascular water protons is achieved by a given CM, a further increase in signal is possible only if extravascular water protons are addressed. Considering this situation, intravascular CM would yield lower signal intensity in the myocardium (for a given CM relaxivity) than extravascular CM. Animal studies demonstrated a reduced dynamic range of myocardial signal response for intravascular CM compared to extravascular CM, which extravasate from the intracapillary compartment during the first pass (36,37). Unfortunately, this situation is not trivial, since intravascular CM, even when confined to the intravascular space, do address "extravascular" water protons through proton exchange (36,37). These mechanisms should be taken into account by perfusion modeling, but have not yet been fully clarified. For more details, see Ref. 38.

Data Analysis

To increase reproducibility and reduce observer-dependence, semiautomatic or automatic analysis procedures for MR perfusion data sets are preferred over manual analysis approaches. Currently, no single analysis algorithm can be identified as the only or best method for detecting CAD. This is not surprising given the large variety of different perfusion imaging protocols and pulse sequences that are currently under evaluation. To allow for better comparisons between different analysis algorithms, at least a common nomenclature for the different approaches would be desirable. A proposed scheme in Figure 4 accounts for two important aspects of analyses: 1) what is being measured, and 2) how the data are extracted. Quantitative analyses yield "quantifiable" perfusion parameters, i.e., parameters that are derived from the signal intensity–time curves according to a well defined mathematical procedure. These parameters are either linked to tissue perfusion or directly represent perfusion in absolute units of mL/min/g tissue. Alternatively, perfusion data analyses can be based on "eyeball" guesses. However, they are often associated with reduced reproducibility (17). It has been shown that semiautomatic data extraction to derive perfusion-linked parameters provides better analysis reproducibility (16).

Parameters Linked to Perfusion

Following correction of the data for motion (caused by imperfect breath-holding) and inhomogeneous coil sensitivity, the peak signal intensity, signal change over time (upslope), arrival time, time to peak signal, mean transit time (MTT), and other parameters can be calculated from signal intensity–time curves (19,20,28,35,39–41). These signal intensity–time curves can be generated on a pixel-by-pixel basis or in segments of various extent and in different layers (e.g., subendocardial and transmural regions).

The upslope of the signal intensity–time curve is most widely used as a quantitative perfusion-linked parameter that closely correlates with microsphere perfusion measurements at relatively low flows (but not high flows) in animal models (40,42) and with PET measurements in humans (26). Further, it uses the initial portion of the signal intensity–time curve (which lasts only a few seconds), which reduces the sensitivity of this parameter for motion (most patients are able to hold their breath for this time period) as well as for CM recirculation.

Analysis of the subendocardial layer, which is known to be most sensitive for perfusion disturbances, is feasible given the high spatial resolution of MR perfusion imaging (26,41,43). An example of a polar map depicting upslope values in the subendocardial layer (i.e., the

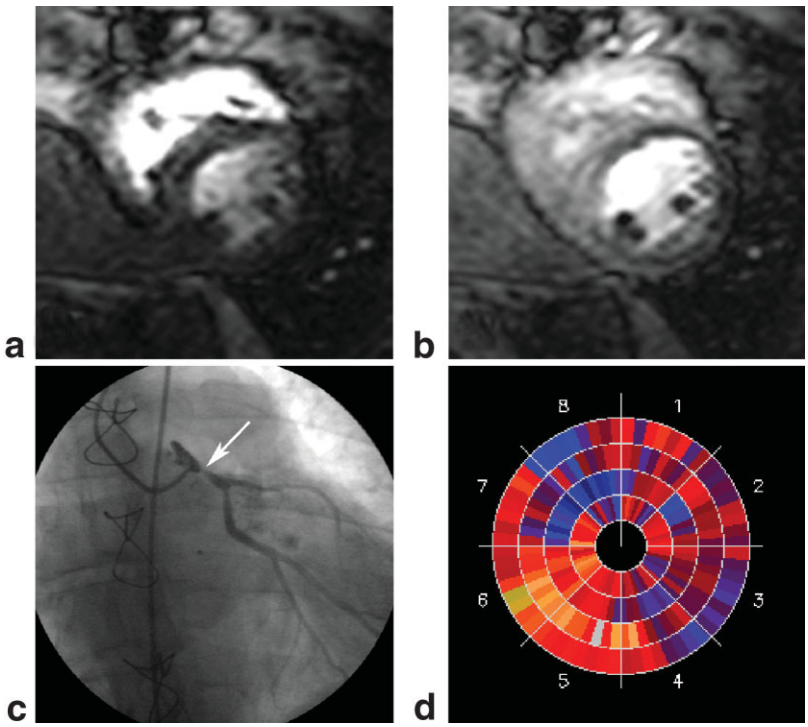

Figure 5. Example of a 43-year-old patient with a history of aortic dissection type A, which was treated with aortic graft surgery. Six months later the exercise test was uneventful, but one year later ST-segment depression occurred together with dyspnea. The perfusion-CMR study (**a:** baseline image; **b:** peak-effect image) demonstrates a large perfusion deficit in the subendocardial layer of the anteroseptal, anterior, anterolateral, and inferolateral walls (i.e., the perfusion territory of the left main coronary artery (**c**)). Only the basal portion of the interventricular septum is normally perfused (no subendocardial dark tissue). The pulse sequence is described in Fig. 1. **d:** A polar map for the upslope values in the subendocardial layer shows approximately three-quarters of the LV myocardium as hypoperfused during adenosine-induced hyperemia. The normal database and the thresholds used for color-coding were established in a recent study (26). Shades of blue represent below-normal perfusion, and shades of red represent normal perfusion (for details see Ref. 26). D. Nanz, Ph.D., is acknowledged for developing the data analysis tools demonstrated in part d.

inner half of the myocardium) is shown in Fig. 5. Such perfusion-linked parameters result in less subjectivity in data interpretation, but require a normal database for comparison. Thus, extracting the perfusion-linked parameters from the data set is only one step, and building a normal database is an important additional effort needed to exploit the advantages of a quantitative approach.

Absolute Perfusion in mL/min/g

In addition to correcting data for coil sensitivity and motion, a quantitative approach also requires conversion of signal intensities into CM concentrations in order to allow for input correction. A prerequisite for such a conversion is an accurate mathematic description of the signal intensity–CM concentration relationship over the full range of CM concentrations that occur in the blood pool and myocardium during first-pass conditions. While a high CNR in the myocardium during first pass is desired, it requires relatively long delay times (between magnetization preparation and readout), and such delay times tend to distort a linear relationship between high blood-pool CM concentrations and signal (42). Thus, specifically designed pulse sequences (44) or a dual-bolus protocol (42) would be required to account for this problem. Once signal intensities have been converted into CM concentrations, different models may be applied to calculate perfusion. Detailed reviews on data analysis and models are available elsewhere (38,45). Models for intravascular CM should take into account proton exchange rates between the vascular and extravascular beds (46), leakage of CM in territories of ischemia (47), and vascular architecture (48). At the present time, the value of a quantitative approach with intravascular CM for detecting CAD in humans is not known.

Diagnostic Performance of Perfusion-CMR

The application of multislice techniques to highly selected patient populations with documented single-vessel disease yielded sensitivities of 100% (22). In a clinical study using a single-slice approach and CM injection into the right atrium, the sensitivity and specificity were 90% and 83%, respectively, for the detection of stenoses ≥75% (24). A study published by our institution (26) using a multislice approach and a peripheral CM injection yielded a sensitivity and specificity of 91% and 94%, respectively, for detection of patients with hemodynamically significant coronary artery stenoses (defined as reduced coronary flow reserve by ^{13}N-ammonia PET). Moreover, the amount of compromised myocardium as assessed by perfusion-CMR (= number of pathological segments) closely agreed with PET measurements. The sensitivity and specificity for detecting morphologically defined CAD (≥1 coronary artery with ≥50% diameter stenosis in quantitative coronary angiography) were as high as 87% and 85%, respectively, even when stenoses of side branches of coronary vessels were considered. In this study, for the detection of anatomically defined CAD, MR yielded an area under the receiver-operator characteristics (ROC) curve (AUC) of 0.91, which compared favorably with 0.93 for PET (corresponding to a sensitivity and specificity of 91% and 81%, respectively). These single-center results were recently confirmed by a multicenter trial (17). Another approach evaluated the potential of semiautomatic analysis of perfusion data for detection of CAD (defined as ≥50% diameter stenosis on quantitative coronary angiography) (16). In this multicenter study we analyzed the slope of the signal intensity–time curve as a perfusion-linked parameter and achieved a sensitivity and specificity of 93% and 75%, respectively, with an AUC of 0.88, confirming the

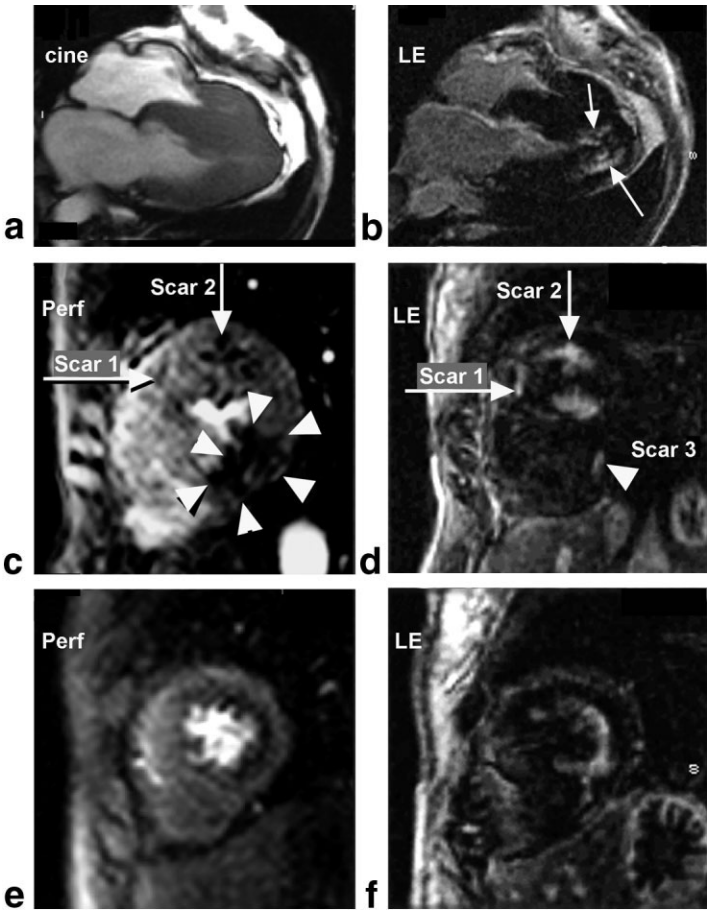

Figure 6. A 35-year-old woman with recurrent chest pain at rest and known hypertrophic cardiomyopathy was referred for a CMR examination. **a:** Cine MR images confirmed hypertrophy of the LV (particularly of the septum) involving the apex of the RV as well. LE-based viability imaging (0.25 mmol/kg Gd-DTPA-BMA) showed considerable scar tissue in the apical region of the LV (arrows in **b**). In a mid-ventricular short-axis slice, first-pass perfusion imaging (0.1 mmol/kg during adenosine 0.14mg/kg/minute over three minutes) shows three hypoperfused areas (**c**). Two of the areas correspond to scar tissue on LE imaging in **d** (arrows: scars 1 and 2), while the largest perfusion deficit in c (arrowheads) resides within viable myocardium with a small central scar region only (arrow head: scar 3 in d). In an apical short-axis slice, first-pass perfusion-CMR (**e**) demonstrates a large subendocardial perfusion deficit involving the anterior, lateral, and inferior walls, which well matches the region of scar tissue on LE imaging (**f**). These findings explain the patient's episodes of chest pain and place her in a higher-risk category due to the scar content (69), and may even indicate progression, since hypoperfused myocardium may be at risk to undergo necrosis in the future.

slope results of the previously-mentioned single-center study (AUC = 0.91) (26).

An even larger multivendor multicenter phase II (dose-finding) clinical trial, known as Magnetic Resonance Imaging for Myocardial Perfusion Assessment in Coronary Artery Disease Trial (MR-IMPACT), was recently finalized. MR-IMPACT involved 234 patients studied in 18 centers worldwide, and confirmed single-center and single-vendor multicenter trials and yielded results superior to SPECT imaging (18). A phase III clinical follow-up trial of MR-IMPACT recently closed recruitment, and analysis is ongoing.

MYOCARDIAL VIABILITY

Once a perfusion abnormality during hyperemic conditions has been detected by perfusion-CMR, it is of major importance to relate this perfusion deficit to either viable (i.e., ischemic myocardium) or scar (i.e., nonviable) tissue. Whereas revascularization should be attempted in the first case, a perfusion deficit related to scar tissue would probably not require any further revascularization. Therefore, it is obvious that in territories with reduced function and the presence of perfusion abnormalities, a viability study should follow to aid in clinical decision-making (i.e., to decide whether revascularization is required or not). T_1-weighted pulse sequences following administration of extravascular Gd-chelates are able to delineate necrotic tissue due to CM accumulation in an extended distribution volume (49). A breakthrough in infarct detection was the introduction of an IR-prepared (and thus heavily T_1-weighted) pulse sequence that yields high signal differences between viable myocardium (with its signal nulled) and scar tissue following Gd-chelate injection (50). With this IR-based late enhancement (LE) technique, infarctions were detected in the acute setting in dogs, and irreversibly damaged myocardium was differentiated from stunned myocardium (51). In patients the LE-based viability imaging was validated in acute (52) and chronic (50) myocardial infarctions. Because of the high spatial resolution of the LE-based viability imaging, it could be shown that both a thickness of viable rim tissue in the subepicardium of $\geq$4 mm and a scar thickness in the subepicardium of $<$4 mm are required to predict functional recovery after revascularization (53). The importance of assessing both perfusion and viability is demonstrated in Fig. 6, which shows a patient with hypertrophic cardiomyopathy. Evaluation of perfusion may also be clinically valuable in patients with a thick RV wall, as seen in pulmonary hypertension or in adult congenital heart disease with RV overload.

ASPECTS OF PERFUSION-CMR TO BE RESOLVED—CHALLENGES FOR THE NEAR FUTURE

During the past 10 years or so, tremendous progress has been achieved with the development of the perfusion-CMR technique in animal experiments (19,20,33,36,40)

and more recently with large international multicenter trials with positive results (16–18). Higher CM doses of extravascular Gd-chelates (ranging from about 0.05 to 0.10 mmol/kg) administered into a peripheral vein with injection rates of about 5 mL/second can be recommended (18). Furthermore, reliable data are now available for fast echo-planar-type readouts with magnetization preparation utilizing a 90° saturation pulse. Nevertheless, many other important issues remain unresolved, and some of these are discussed below. The following paragraphs are therefore meant to stimulate future research. Many questions may be addressed by smaller studies, while other aspects (e.g., robustness of technique, evidence for guidelines, cost-effectiveness, etc.) will primarily require larger multicenter trials.

Stress-Only Protocol vs. Stress-Rest Protocol

For perfusion-CMR, it should be kept in mind that a stress-rest protocol would not be the analog of the conventional scintigraphic approach, which involves administration of radioactive tracers as a stress injection and rest reinjection. In scintigraphy, stress injection is used to probe perfusion, while the rest reinjection probes redistribution of tracer into viable myocytes (i.e., viability), depicting scar tissue as a "cold spot." In analogy, the "rest-injection" in CMR probes redistribution (i.e., scar tissue) by LE imaging (38). Hence, in CMR a stress-only protocol followed by LE imaging is the analog for a SPECT approach.

Some confusion may arise from the fact that in PET, rest-injection of a flow tracer is utilized to measure resting perfusion, which then enters the formula for perfusion reserve calculation. A reduced perfusion reserve is then indicative of the presence of hemodynamically significant stenoses, i.e., CAD (26,54). With this in mind, the stress-rest perfusion approach in CMR could be used to calculate perfusion reserve, as is done in PET, to detect myocardium that is prone to ischemia during increased oxygen demand. For a complete workup involving a stress-rest CMR protocol, additional LE imaging would then be required for viability assessment (for PET, the analog would be the ^{18}F-fluoro-deoxyglucose injection at rest) (53).

Both the stress-only CMR approach (16,26,32) and the stress-rest CMR approach (24,55) have yielded good results for the detection of CAD. It should be kept in mind, however, that a stress-rest approach requires a longer examination time due to the need for two CM injections (and an interval between injection to allow for CM washout), and a longer analysis time (for stress and rest data analysis). Furthermore, it is difficult to match myocardial tissue during stress and rest because the geometry of the heart changes with high heart rates during hyperemia as compared to the resting condition. Most importantly, for perfusion reserve calculations, it must be ensured that a perfusion-related parameter used to calculate perfusion reserve is linearly related to perfusion over a wide range of values, i.e., encompassing resting and hyperemic perfusion (see also absolute quantification of perfusion). Interestingly, in the PET literature the percent area of stenosis on conventional x-ray coronary angiography correlated better with myocardial stress perfusion data than with perfusion reserve data (56–58).

Cardiac Coverage

Extended cardiac coverage would be expected to increase the sensitivity to detect CAD by visualization of smaller areas of hypoperfusion. Furthermore, the extent of perfusion deficits correlates with prognosis. Therefore, an extensive cardiac coverage is clearly advantageous. However, as higher cardiac coverage per unit of time is typically traded for a reduced SNR, CNR, and/or spatial resolution, pulse sequences with an improved cardiac coverage would not necessarily provide a higher diagnostic performance. In this regard, it is noteworthy that several studies demonstrated better diagnostic performance (i.e., higher AUC) when cardiac coverage was reduced by excluding slices with compromised quality (acquired during rapid cardiac motion) (16,32) (see also Fig. 3). However, with the current data, no definite recommendation regarding coverage (i.e., the number of slices) can be made.

Temporal Resolution

Most studies were performed with a temporal resolution of one stack of images acquired every one to two RR-intervals. Some investigators favored a temporal resolution of one stack per RR-interval, while many larger studies with a temporal resolution of one stack per two RR-intervals obtained excellent results with sensitivities and specificities of 87–93% and 75–85%, respectively (16,26). In this regard, higher CM doses yield more points on the upslope of the signal-intensity time curve, and thus compensate for a lower temporal resolution of data acquisition, which can be traded for better cardiac coverage and/or better spatial resolution. Therefore, using higher CM doses with the acquisition of an entire stack every two RR-intervals with consequently better coverage and/or spatial resolution may be advantageous. Because of cardiac mechanics, only one phase in the cardiac cycle (i.e., mid-diastole) has negligible motion, whereas relatively little motion (mostly torsion) is present during late systole (and isovolumetric relaxation). Thus, data acquisition should occur during one or two phases of the cardiac cycle. Accordingly, four slices every two heartbeats can be acquired up to a heart rate of 125/minute using a hybrid echo-planar pulse sequence (with a delay time of 120 msec after the 90° preparation) (26). Using a notch-pulse preparation would allow one to acquire three slices every heartbeat up to a heart rate of 126/minute, or up to seven slices every two heartbeats (16) up to a heart rate of 109/minute, although acquisitions within three or more phases per heartbeat would conflict with the idea of acquiring data during motion-free cardiac phases. This is illustrated in Fig. 3, in which diagnostic performance is diminished for a notched preparation approach when all acquired slices are used for analysis (yielding an AUC of 0.80 for a dose of 0.1 mmol/kg; Fig. 3b), as compared to an analysis based on slices that were primarily acquired during stable cardiac phases (yielding an AUC of 0.91; Fig. 3a) (16).

Pulse Sequence and Field Strength

While hybrid echo-planar sequences can be recommended for perfusion imaging, future large studies are warranted to determine whether parallel imaging strategies with or without SSFP pulse sequences would perform better than hybrid echo-planar readouts. Increasing the field strength from 1.5T to 3T is another way to increase the available magnetization. While diagnostic performance is well documented for 1.5T systems, no comparable data are available for 3T systems, which therefore cannot be recommended at the current time for perfusion imaging. In this context, it should be mentioned that a major advantage of perfusion-CMR over SPECT is that the former provides a high diagnostic performance in all vascular territories (i.e., also in the inferior wall), while the inferior wall in SPECT imaging is susceptible to attenuation artifacts. This important advantage of perfusion-CMR over SPECT should be demonstrated for 3T systems as well, where shimming, particularly of the inferior wall, appears more difficult. In a recent study in volunteers, relative to baseline the increase in myocardial signal during first pass (at 0.1 mmol/kg Gd-DTPA IV) was 2.6 times higher at 3T compared to 1.5T in the anterior wall, but only 1.7 times higher in the inferior wall (59). Larger studies in patients will be needed to show whether an inhomogeneous increase in first-pass signal in different myocardial regions would affect diagnostic performance.

Data Analysis

The question is still open as to whether visual criteria or quantitative parameters (i.e., perfusion-linked or absolute parameters) yield better diagnostic performance. Clearly, a quantitative approach appears advantageous for minimizing observer variability in diagnosis and thus enabling the disease process to be monitored by repetitive perfusion studies. To achieve this goal, analysis software could compare individual patient data with large and representative normal databases to establish the diagnosis. These normal databases, which ideally would be divided into different age and gender categories, should be reestablished if the pulse sequence parameters and/or CM dose or type are changed. Di Bella and coworkers (60) recently demonstrated that the extent of artifacts at the subendocardial border causing reduced signal in the subendocardium not only depends on susceptibility and motion, but also increases with decreasing spatial resolution. This observation underlines the importance of updating normal databases when the pulse sequence parameters are changed.

No definite recommendations can be given at this time regarding the optimum heart model (i.e., the optimum number and position of the segments representing the LV myocardium). The application of a 16- or 17-segment model as recommended for scintigraphy or echocardiography is possible and would allow for comparisons between methods. However, the high spatial resolution achieved by MRI (i.e., the ability to selectively probe the subendocardial layer) would favor a model that includes the subendocardium only. Considering the current slice thicknesses of 8–10 mm, it may be adequate to ignore most apical slices in a short-axis approach to reduce partial-volume artifacts. Such a model could be effective in detecting treatable patients, since the small vessels supplying the apex are typically not amenable to interventions.

Data Quality

Raw data of high quality are essential for any reliable analysis approach. Visual analysis exploits the ability of an experienced reader to compensate for inadequate quality, but is traded for lower reproducibility unless strict reading criteria are defined. For semiautomatic and particularly for automatic analyses, adequate data quality is crucial, as shown by multicenter data (Fig. 3) (16). Therefore, definitions of quantifiable quality criteria will be needed in the future to improve on this aspect of perfusion-CMR.

FUTURE PERSPECTIVES

As demonstrated by a substantial number of single-center studies and more recently by large multicenter studies, perfusion-CMR may become a first-line modality in the workup of patients with known or suspected CAD in the near future. In patients with wall motion abnormalities, the combined approach of perfusion-CMR and LE-CMR appears particularly attractive for a comprehensive workup of cardiac patients. Since perfusion-CMR is free of radiation, this technique may be particularly useful for adult congenital heart disease after coronary artery surgery (e.g., after a switch operation) or in patients with a history of Kawasaki disease, for whom monitoring of disease over many decades is required (61).

Shift in the Paradigm: From a Reactive to an Active Strategy

During the last decade, remarkable progress in the field of interventional cardiology has been achieved with steadily increasing success in revascularizations even in the setting of acute coronary syndrome or acute myocardial infarction. Nevertheless, approximately 60% of cardiac deaths occur before the patients reach the catheterization laboratory for treatment (62). These circumstances indicate an insufficient diagnostic approach in clinical cardiac routines. Typically, patients are identified as being at risk when they are symptomatic for angina, dyspnea, or arrhythmias. To detect patients at risk for myocardial infarction more efficiently, an active strategy could be pursued whereby patients are approached for CAD detection by perfusion-CMR before symptoms occur. The selection of patients to undergo such a CMR evaluation, and the choice of monitoring strategy could be based on their global cardiovascular risk. Today, global risk is generally estimated by considering the classic risk factors (63–65). In addition, vascular function assessments (e.g., by fast MR techniques (66)) could add valuable information, and individual characterization of gene patterns (67,68) could further define individual cardiovascular risk. It will be a challenge for upcoming perfusion-CMR trials

to provide supportive data for such a risk-based role of perfusion-CMR in the future.

REFERENCES

1. Yusuf S, Hawken S, Ounpuu S, et al. Effect of potentially modifiable risk factors associated with myocardial infarction in 52 countries (the INTERHEART study): case-control study [see comment]. Lancet 2004;364:937–952.
2. Naghavi M, Libby P, Falk E, et al. From vulnerable plaque to vulnerable patient: a call for new definitions and risk assessment strategies: Part I. Circulation 2003;108:1664–1672.
3. Ambrose JA, Tannenbaum MA, Alexopoulos D, et al. Angiographic progression of coronary artery disease and the development of myocardial infarction. J Am Coll Cardiol 1988;12:56–62.
4. Little WC, Constantinescu M, Applegate RJ, et al. Can coronary angiography predict the site of a subsequent myocardial infarction in patients with mild-to-moderate coronary artery disease? Circulation 1988;78(5 Pt 1):1157–1166.
5. Giroud D, Li JM, Urban P, Meier B, Rutishauser W. Relation of the site of acute myocardial infarction to the most severe coronary arterial stenosis at prior angiography. Am J Cardiol 1992;69:729–732.
6. Kemp HG, Kronmal RA, Vlietstra RE, Frye RL. Seven year survival of patients with normal or near normal coronary arteriograms: a CASS registry study. J Am Coll Cardiol 1986;7:479–483.
7. Bruschke AV, Kramer Jr JR, Bal ET, Haque IU, Detrano RC, Goormastic M. The dynamics of progression of coronary atherosclerosis studied in 168 medically treated patients who underwent coronary arteriography three times. Am Heart J 1989;117:296–305.
8. Ellis S, Alderman E, Cain K, Fisher L, Sanders W, Bourassa M. Prediction of risk of anterior myocardial infarction by lesion severity and measurement method of stenoses in the left anterior descending coronary distribution: a CASS Registry Study. J Am Coll Cardiol 1988;11:908–916.
9. Waters D, Lesperance J, Francetich M, et al. A controlled clinical trial to assess the effect of a calcium channel blocker on the progression of coronary atherosclerosis. Circulation 1990;82:1940–1953.
10. Ojio S, Takatsu H, Tanaka T, et al. Considerable time from the onset of plaque rupture and/or thrombi until the onset of acute myocardial infarction in humans: coronary angiographic findings within 1 week before the onset of infarction. Circulation 2000;102:2063–2069.
11. Iskander S, Iskandrian AE. Risk assessment using single-photon emission computed tomographic technetium-99m sestamibi imaging. J Am Coll Cardiol 1998;32:57–62.
12. Seiler C, Kirkeeide RL, Gould KL. Measurement from arteriograms of regional myocardial bed size distal to any point in the coronary vascular tree for assessing anatomic area at risk. J Am Coll Cardiol 1993;21:783–797.
13. Fung AY, Gallagher KP, Buda AJ. The physiologic basis of dobutamine as compared with dipyridamole stress interventions in the assessment of critical coronary stenosis. Circulation 1987;76:943–951.
14. Cerqueira M, Verani M, Schwaiger M, Heo J, Iskandrian A. Safety profile of adenosine stress perfusion imaging: results from the Adenoscan Multicenter Trial Registry. J Am Coll Cardiol 1994;23:384–389.
15. Marwick T, Willemart B, D'Hondt AM, et al. Selection of the optimal nonexercise stress for the evaluation of ischemic regional myocardial dysfunction and malperfusion. Comparison of dobutamine and adenosine using echocardiography and 99mTc-MIBI single photon emission computed tomography. Circulation 1993;87:345–354.
16. Giang T, Nanz D, Coulden R, et al. Detection of coronary artery disease by magnetic resonance myocardial perfusion imaging with various contrast medium doses: first European multicenter experience. Eur Heart J 2004;25:1657–1665.
17. Wolff S, Schwitter J, Coulden R, et al. Myocardial first-pass perfusion magnetic resonance imaging: a multicenter dose-ranging study. Circulation 2004;110:732–737.
18. Schwitter J, Bauer W, van Rossum A, et al. MR-IMPACT: comparison of myocardial perfusion imaging with single photon emission computed tomography in known or suspected coronary artery disease: a multicentre, multivendor dose finding study. Eur Heart J 2005 (supplement, abstract).
19. Saeed M, Wendland MF, Sakuma H, et al. Coronary artery stenosis: detection with contrast-enhanced MR imaging in dogs. Radiology 1995;196:79–84.
20. Schwitter J, Saeed M, Wendland MF, et al. Assessment of myocardial function and perfusion in a canine model of non-occlusive coronary artery stenosis using fast magnetic resonance imaging. J Magn Reson Imaging 1998;9:101–110.
21. Manning WJ, Atkinson DJ, Grossman W, Paulin S, Edelman RR. First-pass nuclear magnetic resonance imaging studies using gadolinium-DTPA in patients with coronary artery disease. J Am Coll Cardiol 1991;18:959–965.
22. Lauerma K, Virtanen KS, Sipila LM, Hekali P, Aronen HJ. Multislice MRI in assessment of myocardial perfusion in patients with single-vessel proximal left anterior descending coronary artery disease before and after revascularization. Circulation 1997;96:2859–2867.
23. Matheijssen NA, Louwerenburg HW, van Rugge F, et al. Comparison of ultrafast dipyridamole magnetic resonance imaging with dipyridamole sestamibi SPECT for detection of perfusion abnormalities in patients with one-vessel coronary artery disease: assessment by quantitative model fitting. Magn Reson Med 1996;35:221–228.
24. Al-Saadi N, Nagel E, Gross M, et al. Noninvasive detection of myocardial ischemia from perfusion reserve based on cardiovascular magnetic resonance. Circulation 2000;101:1379–1383.
25. Elkington AG, Gatehouse PD, Cannell TM, et al. Comparison of hybrid echo-planar imaging and FLASH myocardial perfusion cardiovascular MR imaging. Radiology 2005;235:237–243.
26. Schwitter J, Nanz D, Kneifel S, et al. Assessment of myocardial perfusion in coronary artery disease by magnetic resonance: a comparison with positron emission tomography and coronary angiography. Circulation 2001;103:2230–2235.
27. Schreiber WG, Schmitt M, Kalden P, Mohrs OK, Kreitner KF, Thelen M. Dynamic contrast-enhanced myocardial perfusion imaging using saturation-prepared TrueFISP. J Magn Reson Imaging 2002;16:641–652.
28. Klocke FJ, Simonetti OP, Judd RM, et al. Limits of detection of regional differences in vasodilated flow in viable myocardium by first-pass magnetic resonance perfusion imaging. Circulation 2001;104:2412–2416.
29. Pruessmann KP, Weiger M, Scheidegger MB, Boesiger P. SENSE: sensitivity encoding for fast MRI. Magn Reson Med 1999;42:952–962.
30. Kellman P, Derbyshire JA, Agyeman KO, McVeigh ER, Arai AE. Extended coverage first-pass perfusion imaging using slice-interleaved TSENSE. Magn Reson Med 2004;51:200–204.
31. Kostler H, Sandstede JJ, Lipke C, Landschutz W, Beer M, Hahn D. Auto-SENSE perfusion imaging of the whole human heart. J Magn Reson Imaging 2003;18:702–708.
32. Bertschinger KM, Nanz D, Buechi M, et al. Magnetic resonance myocardial first-pass perfusion imaging: parameter optimization for signal response and cardiac coverage. J Magn Reson Imaging 2001;14:556–562.
33. Saeed M, Wendland M, Yu K, Li H, Higgins C. Dual effects of gadodiamide injection in depiction of the region of myocardial ischemia. J Magn Reson Imaging 1993;3:21–29.
34. Wilke N, Kroll K, Merkle H, et al. Regional myocardial blood volume and flow: first-pass MR imaging with polylysine-Gd-DTPA. J Magn Reson Imaging 1995;5:227–237.
35. Kraitchman DL, Chin BB, Heldman AW, Solaiyappan M, Bluemke DA. MRI detection of myocardial perfusion defects due to coronary artery stenosis with MS–325. J Magn Reson Imaging 2002;15:149–158.
36. Wendland MF, Saeed M, Yu KK, et al. Inversion recovery EPI of bolus transit in rat myocardium using intravascular and extravascular gadolinium-based MR contrast media: dose effects on peak signal enhancement. Magn Reson Med 1994;32:319–329.
37. Judd RM, Atalay MK, Rottman GA, Zerhouni EA. Effects of myocardial water exchange on T1 enhancement during bolus administration of MR contrast agents. Magn Reson Med 1995;33:215–223.
38. Schwitter J. Myocardial perfusion in ischemic heart disease. In: Higgins CB, de Roos A, editors. MRI and CT of the cardiovascular system. 2nd ed: Philadelphia, PA, Lippincott Williams and Wilkins; 2005.

39. Keijer JT, van Rossum A, van Eenige M, et al. Semiquantitation of regional myocardial blood flow in normal human subjects by first-pass magnetic resonance imaging. Am Heart J 1995;130:893–901.
40. Wilke N, Simm C, Zhang J, et al. Contrast-enhanced first pass myocardial perfusion imaging: correlation between myocardial blood flow in dogs at rest and during hyperemia. Magn Reson Med 1993;29:485–497.
41. Panting JR, Gatehouse PD, Yang GZ, et al. Abnormal subendocardial perfusion in cardiac syndrome X detected by cardiovascular magnetic resonance imaging. N Engl J Med 2002;346:1948–1953.
42. Christian TF, Rettmann DW, Aletras AH, et al. Absolute myocardial perfusion in canines measured by using dual-bolus first-pass MR imaging. Radiology 2004;232:677–684.
43. Keijer JT, van Rossum AC, van Eenige MJ, et al. Magnetic resonance imaging of regional myocardial perfusion in patients with single-vessel coronary artery disease: quantitative comparison with (201)Thallium-SPECT and coronary angiography. J Magn Reson Imaging 2000;11:607–615.
44. Gatehouse PD, Elkington AG, Ablitt NA, Yang GZ, Pennell DJ, Firmin DN. Accurate assessment of the arterial input function during high-dose myocardial perfusion cardiovascular magnetic resonance. J Magn Reson Imaging 2004;20:39–45.
45. Kroll K, Wilke N, Jerosch Herold M, et al. Modeling regional myocardial flows from residue functions of an intravascular indicator. Am J Physiol 1996;271 (4 Pt 2):H1643–1655.
46. Judd RM, Reeder SB, May Newman K. Effects of water exchange on the measurement of myocardial perfusion using paramagnetic contrast agents. Magn Reson Med 1999;41:334–342.
47. Dauber IM, VanBenthuysen KM, McMurtry IF, et al. Functional coronary microvascular injury evident as increased permeability due to brief ischemia and reperfusion. Circ Res 1990;66:986–998.
48. Weisskoff RM, Chesler D, Boxerman JL, Rosen BR. Pitfalls in MR measurement of tissue blood flow with intravascular tracers: which mean transit time? Magn Reson Med 1993;29:553–558.
49. Schwitter J, Saeed M, Wendland MF, et al. Influence of severity of myocardial injury on distribution of macromolecules: extravascular versus intravascular gadolinium-based magnetic resonance contrast agents. J Am Coll Cardiol 1997;30:1086–1094.
50. Kim RJ, Wu E, Rafael A, et al. The use of contrast-enhanced magnetic resonance imaging to identify reversible myocardial dysfunction. N Engl J Med 2000;343:1445–1453.
51. Hillenbrand HB, Kim RJ, Parker MA, Fieno DS, Judd RM. Early assessment of myocardial salvage by contrast-enhanced magnetic resonance imaging. Circulation 2000;102:1678–1683.
52. Choi KM, Kim RJ, Gubernikoff G, Vargas JD, Parker M, Judd RM. Transmural extent of acute myocardial infarction predicts long-term improvement in contractile function. Circulation 2001;104: 1101–1107.
53. Knuesel PR, Nanz D, Wyss C, et al. Characterization of dysfunctional myocardium by positron emission tomography and magnetic resonance: relation to functional outcome after revascularization. Circulation 2003;108:1095–1100.
54. Schwaiger M. Myocardial perfusion imaging with PET. J Nucl Med 1994;35:693–698.
55. Cullen JH, Horsfield MA, Reek CR, Cherryman GR, Barnett DB, Samani NJ. A myocardial perfusion reserve index in humans using first-pass contrast-enhanced magnetic resonance imaging. J Am Coll Cardiol 1999;33:1386–1394.
56. Uren NG, Melin JA, De Bruyne B, Wijns W, Baudhuin T, Camici PG. Relation between myocardial blood flow and the severity of coronary artery stenosis. N Engl J Med 1994;330:1782–1788.
57. Di Carli M, Czernin J, Hoh CK, et al. Relation among stenosis severity, myocardial blood flow, and flow reserve in patients with coronary artery disease. Circulation 1995;91:1944–1951.
58. Sambuceti G, Parodi O, Marcassa C, et al. Alterations in regulation of myocardial blood flow in one-vessel coronary artery disease determined by positron emission tomography. Am J Cardiol 1993;72: 538–543.
59. Araoz PA, Glockner JF, GcGee KP, et al. 3 Tesla MR imaging provides improved contrast in first-pass myocardial perfusion imaging over a ragne of gadolinium doses. J Cardiovasc Magn Reson 2005; 7:559–564.
60. Di Bella EVR, Parker DL, Sinusas AJ. On the dark rim artifact in dynamic contrast-enhanced MRI myocardial perfusion studies. Magn Reson Med 2005.
61. Valsangiacomo Buechel E, Bauersfeld U, Kellenberger C, Schwitter J. Evaluation of myocardial perfusion by MRI in children with congenital or acquired coronary artery disease [Abstract]. J Cardiovasc Magn Reson 2006;8:25.
62. American Heart Association. Heart disease and stroke statistics: update 2006. Circulation 2006; e85–e151.
63. Assmann G, Cullen P, Schulte H. Simple scoring scheme for calculating the risk of acute coronary events based on the 10-year follow-up of the prospective cardiovascular Munster (PROCAM) study. Circulation 2002;105:310–315.
64. Wilson PW, D'Agostino RB, Levy D, Belanger AM, Silbershatz H, Kannel WB. Prediction of coronary heart disease using risk factor categories. Circulation 1998;97:1837–1847.
65. Conroy RM, Pyorala K, Fitzgerald AP, et al. Estimation of ten-year risk of fatal cardiovascular disease in Europe: the SCORE project [see comment]. Eur Heart J 2003;24:987–1003.
66. Schwitter J, Oelhafen M, Wyss BM, et al. 2D-spatially-selective real-time magnetic resonance imaging for the assessment of microvascular function and its relation to the cardiovascular risk profile. J Cardiovasc Magn Reson 2006;8:759–769.
67. Yamada Y, Izawa H, Ichihara S, et al. Prediction of the risk of myocardial infarction from polymorphisms in candidate genes. N Engl J Med 2002;347:1916–1923.
68. Topol E, McCarthy J, Gabriel S, et al. Single nucleotide polymorphisms in multiple novel thrombospondin genes may be associated with familial premature myocardial infarction. Circulation 2001; 104:2641–2644.
69. Moon J, McKenna W, McCrohon J, Elliott P, Smith G, Pennell D. Toward clinical risk assessment in hypertrophic cardiomyopathy with gadolinium cardiovascular Magnetic Resonance. J Am Coll Cardiol 2003;41:1561–1567.
70. Schwitter J. CMR of myocardial perfusion. In: Lardo AC, Fayad ZA, Chronos NAF, Fuster V, editors. Cardiovascular magnetic resonance: established and emerging applications. New York: Martin Dunitz, Taylor & Francis; 2003.